

See discussions, stats, and author profiles for this publication at: <https://www.researchgate.net/publication/263982582>

Optical Properties of Gold Nanorattles: Evidences for Free Movement of the Inside Solid Nanosphere

ARTICLE *in* THE JOURNAL OF PHYSICAL CHEMISTRY C · MAY 2014

Impact Factor: 4.77 · DOI: 10.1021/jp502236e

CITATIONS

4

READS

34

1 AUTHOR:



Mahmoud A. Mahmoud

Georgia Institute of Technology

76 PUBLICATIONS 1,807 CITATIONS

[SEE PROFILE](#)

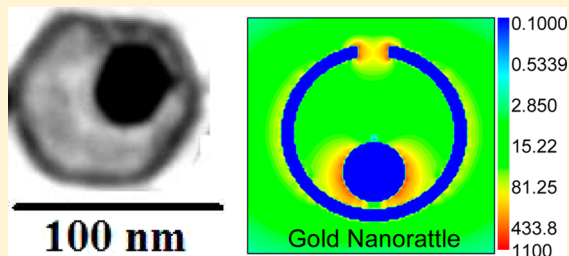
Optical Properties of Gold Nanorattles: Evidences for Free Movement of the Inside Solid Nanosphere

Mahmoud A. Mahmoud*

Laser Dynamics Laboratory, School of Chemistry and Biochemistry, Georgia Institute of Technology, Atlanta, Georgia 30332-0400, United States

 Supporting Information

ABSTRACT: Gold nanorattles (AuNRTs), hollow gold nanospheres with internal small solid gold nanospheres (AuNSs), were prepared with different sizes. The presence of AuNS inside the hollow gold nanospheres in the nanorattle shape was found to improve their sensing efficiency. The sensitivity factor of the nanorattles is in the range of 450 nm/RIU, while the individual hollow nanosphere's efficiency is \sim 300 nm/RIU. This improvement is due to the strong plasmon field on the cavity and around the inner gold nanosphere as shown by using the discrete dipole approximation (DDA) calculations. Interestingly, this nanoparticle produces a strong enhancement for the interaction of light at 850 nm due to the excitation of both the inner sphere and outer nanoshell, despite being the fact that NIR radiation (850 nm) has very low energy to excite the inner gold nanosphere when present alone. Comparing the experimental and simulated scattering spectrum for a single colloidal nanorattle suggests that the interior gold nanosphere moves freely inside the gold nanoshell. When the rattle is dried, the nanosphere adheres to the inner surface as shown from the experimental and theoretical results. Unlike nanospheres and nanoshells, the nanorattles have three plasmon peaks in addition to a shoulder. This allows the AuNRTs to be useful in applications in the visible and near IR spectral regions.



INTRODUCTION

When the conduction band free electrons of plasmonic nanoparticles interact with electromagnetic radiation of resonance frequency, they oscillate collectively producing an electromagnetic plasmon field.^{1,2} This plasmon field enhances both the absorption and scattering of resonant photons. The absorption and scattering spectra together comprise the localized surface plasmon resonance (LSPR) extinction spectrum.³ The resonance frequencies (LSPR peak positions) of the plasmonic nanoparticles depend on their shape, size, and dielectric constant of the material and its surrounding.⁴ Since the dielectric function of the surrounding medium also affects the LSPR spectrum, these particles could be used for sensing.⁵ The sensitivity factor of the plasmonic nanoparticles is defined as the ratio between the change of the value of the plasmon peak position and the change in the refractive index of the surrounding medium ($SF = \Delta\lambda/\Delta n$) with units of nm/RIU.⁶ The sensitivity factors of many shapes and types of plasmonic nanoparticles have been measured including gold nanospheres,⁷ gold nanocubes,⁷ gold nanorods,⁷ hexagonal silver arrays,⁸ silver nanocubes,⁹ hollow gold nanospheres, hollow gold nanocages,¹⁰ gold nanoframes,¹¹ and nanorice¹² with sensitivity factors (SF) of 44,⁷ 83,⁷ 150–285,⁷ 191,⁸ 113 \pm 5,⁹ 298 \pm 7,⁴⁰⁸,¹⁰ 620,¹¹ and 801¹² nm/RIU, respectively.

The number of LSPR peaks depends on the shape of the plasmonic nanoparticles. Symmetrical nanoparticles with shapes such as spheres,¹³ cubes,¹⁴ hexagon,¹⁴ rectangle,¹⁴ and octahedral¹⁵ have one plasmon peak, while asymmetric shapes

such as nanorods,¹⁶ nanostar,¹⁷ rice,¹² plates,¹⁸ and bars¹⁹ show more than one plasmon peak. The advantage of presence of multiple plasmon peaks is that it extends the coverage of the nanoparticle for applications. Since the fluidic diffusion of the nanoparticles and the cellular uptake in biology depend greatly on the shape of the nanoparticles, symmetrical shapes are characterized by the good diffusibility, it will be useful to prepare plasmonic nanoparticles of symmetrical shape with more than one LSPR peak for such applications.

Nanorattles consisting of gold and silver nanoalloy cores and gold and silver alloy nanoshells were fabricated by the galvanic replacement technique, gold and silver alloy nanoparticles was used as a template.²⁰ The aim of this work is to prepare gold nanorattles of different dimensions (size of the inside gold nanosphere and the outer gold nanoshell) by a simple approach. The optical properties of the nanorattles are studied experimentally and theoretically by the discrete dipole approximation (DDA). Comparing the experimental and the simulated results make it possible to prove the free movement of the nanosphere inside the gold nanoshell. The DDA simulation showed that the plasmon field is distributed with high intensity around both the inside gold nanosphere as well as the outside gold nanoshell. This explains the high sensitivity factors of the gold nanorattles compared to gold nanoshells.

Received: March 4, 2014

Revised: April 25, 2014

Published: April 28, 2014



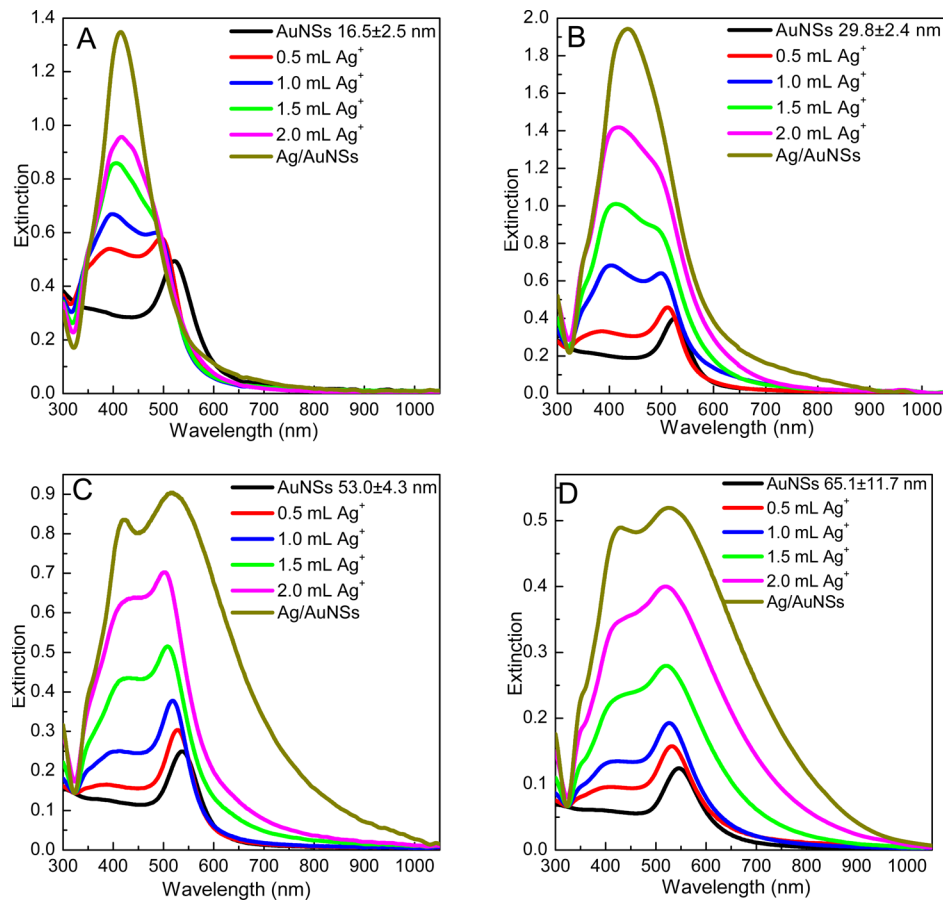


Figure 1. Localized surface plasmon resonance extinction spectra of gold nanospheres (AuNSs) and AuNSs coated with silver nanoshells of different thicknesses resulting from the reduction of different amounts of silver nitrate on the surface of AuNSs. The LSPR peak corresponding to the silver nanoshell, which appears at higher energy, increases with increasing the thickness of silver nanoshell. The diameter of AuNCs is (A) 16.5 ± 2.5 , (B) 29.8 ± 2.4 , (C) 53.0 ± 4.3 , and (D) 65.1 ± 11.7 nm.

EXPERIMENT

Gold nanorattles (AuNRTs) were prepared by the galvanic replacement technique.²¹ The silver atoms in gold–silver core–shell nanospheres were replaced with gold to produce nanoshells. Gold nanospheres (AuNSs) were prepared by the citrate reduction approach²² with citrate used as capping agent as well.²² The size of the gold nanospheres was reduced by increasing the amount of citrate salt added during the synthesis. Briefly, 150 mL of 1% hydrogentetrachloroaurate trihydrate ($\text{HAuCl}_4 \cdot 3\text{H}_2\text{O}$, Sigma-Aldrich) aqueous solution was brought to boiling, and 3 mL of sodium citrate trihydrate (Sigma-Aldrich) of concentration of 2, 1, 0.3, or 0.2 % were added. The solution was heated and stirred until it turned the color of red wine. The solution of the AuNSs was allowed to cool down. The AuNSs were cleaned from the byproducts especially the chloride ions by twice centrifugation at 9000 rpm for 5 min and redispersion in DI water. Finally, the nanoparticles were dispersed in DI water.

In order to prepare gold–silver core–shell nanoparticles (Au–Ag NSs), the cleaned AuNSs was diluted by DI water until optical density of 0.5, 0.4, 0.25, and 0.125 for the samples prepared by citrate concentration of 2, 1, 0.3, or 0.2%, respectively. A 125 mL sample of AuNSs solution was brought to boiling and 4 mL of sodium citrate trihydrate (0.068 M) and 2 mL silver nitrate (0.117 M) were added. The citrate and silver nitrate solutions were added to 1 mL citrate followed by 0.5 mL silver salt every 2 min. The solution was boiled and stirred for

another 2 min until it turned yellow for the first two samples or opaque for the other two samples, finally 0.05 g polyvinylpyrrolidone (PVP, MW = 55 000) dissolved in 5 mL of DI water was added.

AuNRTs were prepared from Ag-AuNSs as follows: a 50 mL solution of Ag-AuNSs was cleaned, by centrifugation at 5 000 rpm for 5 min, and dispersed in 100 mL of DI water. Then, 0.05 g of PVP dissolved in 5 mL DI water was added. The final solution was heated to 80 °C. Under stirring, $\text{HAuCl}_4 \cdot 3\text{H}_2\text{O}$ (0.001 g/10 mL) aqueous solution was added dropwise until the LSPR peak shifted from ~400 to ~800 nm. The AuNRTs solution kept undisturbed for 24 h to allow the AgCl precipitate to settle. Then, the clean AuNRTs were decanted from the precipitate. A 10 mL sample of AuNRTs was cleaned by centrifugation at 6000 rpm for 10 min and the residue was redispersed in 2 mL of ethanol. In order to measure the sensitivity factors, the AuNRTs were centrifugation at 4000 rpm for 10 min and the residue was redispersed in different solvents such as water, methanol, ethanol, dichloromethane, chloroform, and carbon tetrachloride. The LSPR extinction spectrum was measured by an Ocean Optics HR4000Cg-UV-NIR. A JEOL 100C transmission electron microscope (TEM) was used to characterize the prepared nanoparticles. CytoViva Hyperspectral microabsorption spectrometer system was used for the single particle scattering spectral measurement.

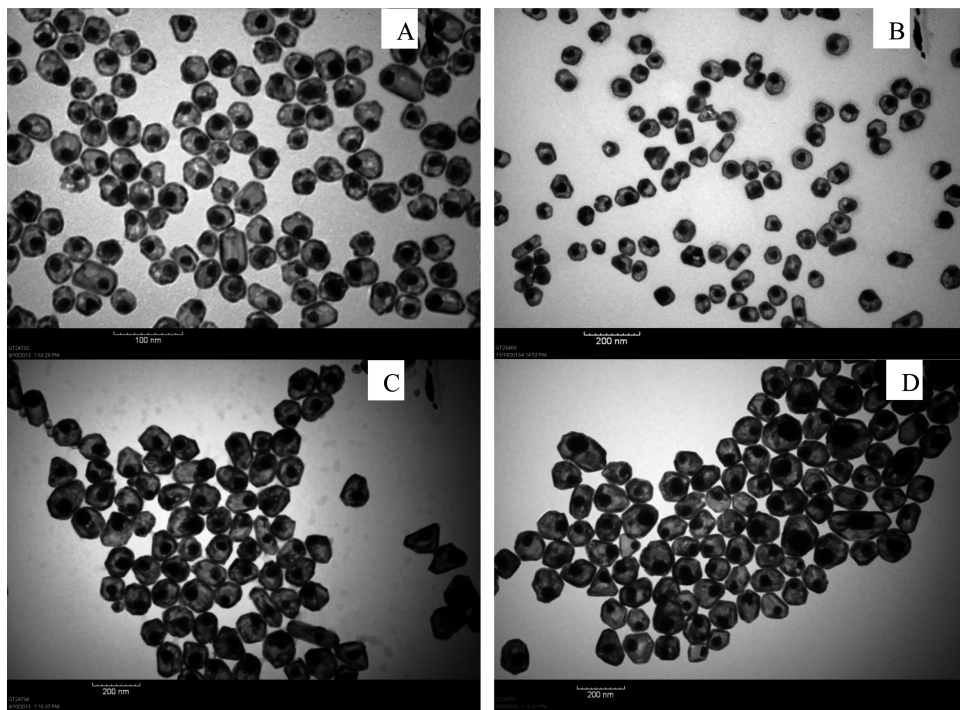


Figure 2. TEM images of gold nanorattles with inside gold nanosphere and outer gold nanoshell of different dimensions: (A) 16.5 ± 2.5 nm inside spheres and 47.4 ± 5.4 nm outer gold shell, (B) 29.8 ± 2.4 nm inside spheres and 85.1 ± 7.3 nm outer shells, (C) 53.0 ± 4.3 nm inside spheres and 143.4 ± 16.9 nm outer shells, and (D) 65.1 ± 11.7 nm inside spheres and 158.6 ± 23.2 nm outer shells.

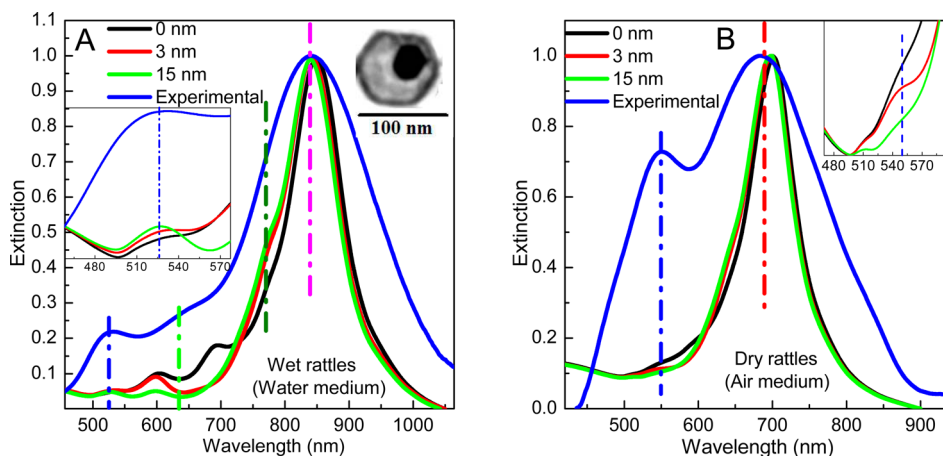


Figure 3. Surface plasmon resonance spectra of a single gold nanorattle of 30 nm inside AuNSs (90 nm shell) measured and calculated in (A) water medium and (B) air medium. The experimental result (blue), calculated spectrum carried out by the DDA technique at a separation distance of 0 (black), 3 (red), and 15 nm (green). Both the experimental measurement and theoretical calculation are carried out on the surface of silicon coated with oxide layer substrate. The incident field is polarized parallel to the surface of the substrate. The inset spectrum in each figure is a magnification of the LSPR spectrum around 500 nm. The inset SEM image in part A is for a single AuNRT: that its LSPR scattering is measured by the single particle setup.

RESULTS AND DISCUSSION

Optical Properties of Gold–Silver Core–Shell Nanoparticles. Combining two metals in the nanoscale either by alloying,²³ core–shell,²⁴ hollow double shell,²⁵ or selective coating^{26,27} structure changes the electronic, optical, mechanical, and catalytic properties of the nanostructures. Although the presence of more than one metal in one nanoparticle could enhance some of its properties, it could also have a negative effect on the other properties. Coating gold nanospheres with silver nanoshells is an intermediate step during the synthesis of AuNRTs; it is worth studying the gold–silver core–shell

nanostructures because they are potentially useful in many optical applications.

In order to grow a nanoshell of a metal on the surface of a certain nanoparticle, the following effects should be considered: the lattice matching between the two metals, the capping materials compatibility with the two metals, and the rate of reduction of ions and diffusion of atoms compared with the rate of crystallization of the atoms on the nanoparticles' facets. In a typical synthesis of core–shell Au–AgNSs, gold nanospheres are prepared first by citrate reduction. Citrate in this case is the reducing and capping agent, which does the same function for the silver nanoshell. Moreover, the lattice parameters of both

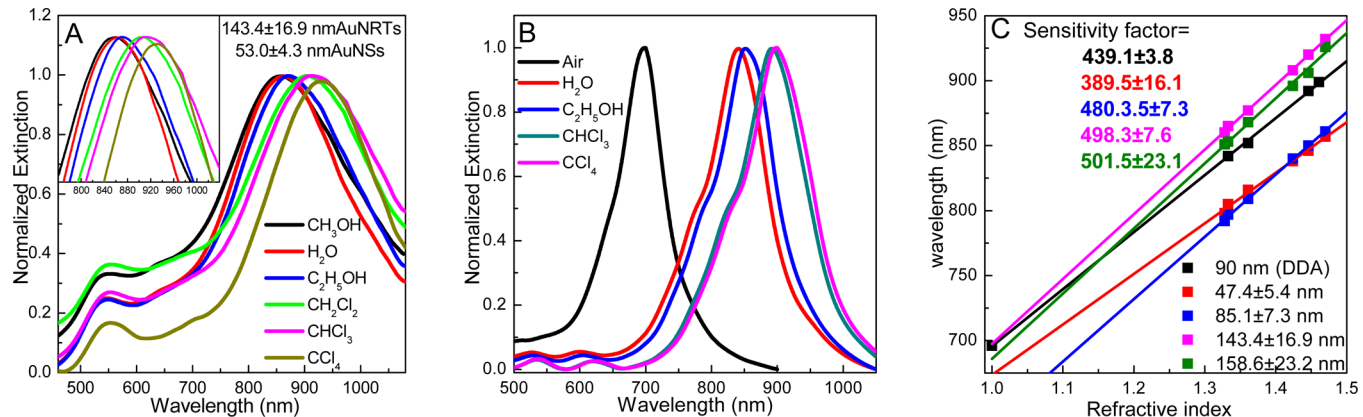


Figure 4. (A) LSPR spectra of 143.4 ± 16.9 nm AuNRTs of 53.0 ± 4.3 nm interior AuNSs, measured when dispersed in different solvents, red shift as the refractive index of the solvent is increased, the inset is magnification for the top of the spectrum. (B) LSPR spectrum of 90 nm AuNRT of 30 nm inside AuNS and 6 nm wall thickness, calculated by DDA technique in different solvent dielectrics. (C) Relationship between the value of the LSPR peak position of AuNRTs of different sizes (inner gold nanosphere and outer gold hollow nanosphere) and the refractive index of the surrounding solvent. The slope of this linear relationship is the sensitivity factor.

Table 1. Sensitivity Factor of Gold Nanorattles with Different Sizes of Inner Gold Nanosphere and Outer Gold Hollow Nanospheres

gold nanorattles		
outer shell (nm)	inner sphere (nm)	sensitivity factor (nm/RIU)
90 ^a	30 ^a	439.1 ± 3.8 ^a
47.4 ± 5.4	16.5 ± 2.5	389.5 ± 16.1
85.1 ± 7.3	29.8 ± 2.4	480.3 ± 7.3
143.4 ± 16.9	53.0 ± 4.3	498.3 ± 7.6
158.6 ± 23.2	65.1 ± 11.7	501.5 ± 23.1

^aSimulated by DDA technique.

gold and silver are comparable; this lattice matching allows uniformly growth of silver atoms on the surface of AuNCs making the outer shape spherical too. Parts A–D of Figure 1 show the LSPR extinction spectra of AuNSs with diameters of 16.5 ± 2.5 , 29.8 ± 2.4 , 53.0 ± 4.3 , and 65.1 ± 11.7 nm (TEM images are shown in Figure S1, Supporting Information), respectively, before and after coating with different amounts of silver nanoshell. Silver nitrate of different amounts is reduced on the surface of AuNSs. In case of the four different sizes of AuNSs, when silver is deposited on the surface of AuNSs, a new plasmon band at higher energy appeared and the LSPR corresponding to the AuNSs is shifted to higher energy. As the amount of silver is increased the intensity of the peak at the

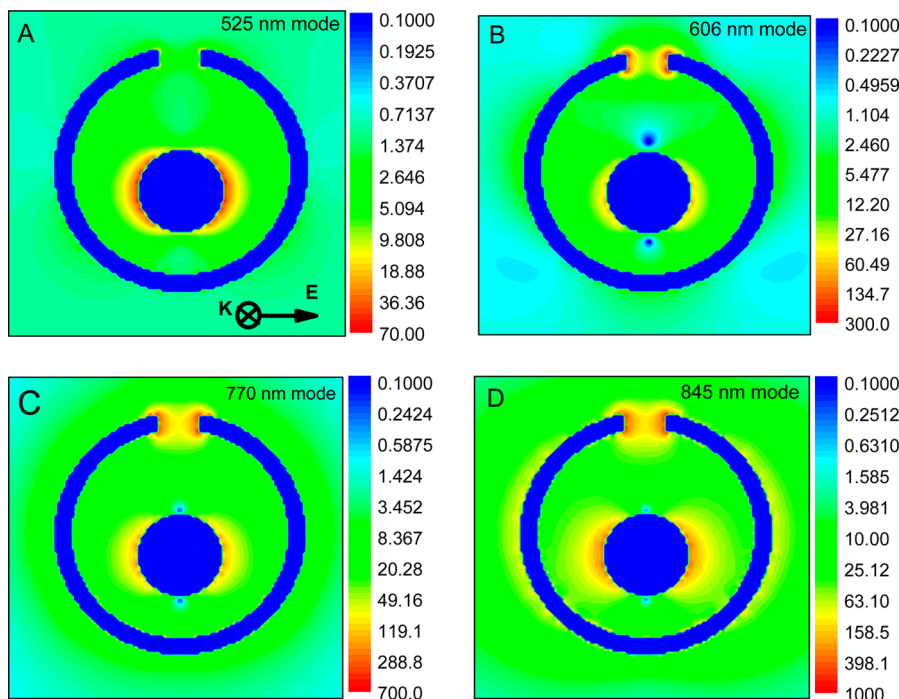


Figure 5. Plasmon field distribution counter for 90 nm gold nanorattle of 6 nm wall thickness and 30 nm inside AuNS calculated by DDA technique at plasmon mode of (A) 525, (B) 606, (C) 770, and (D) 845 nm. It is clear that the 845 nm mode is the most efficient one, since the field strength is the highest and the field is distributed around both the inside AuNS nanoshell and the outer nanoshell.

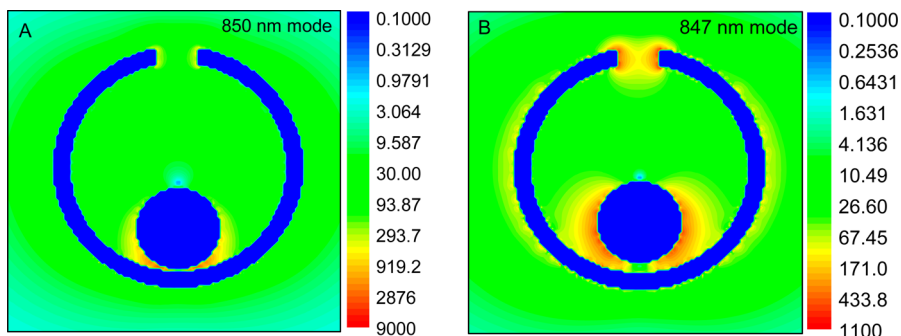


Figure 6. Plasmon field distribution contours of 90 nm gold nanorattle of 6 nm thickness and 30 nm inside gold nanosphere, calculated by DDA when the inside separation gap between the nanosphere and the shell is (A) 0 nm for 850 nm plasmon mode and (B) 3 nm for 847 nm plasmon mode. The field intensity increases as the separation gap is decreased at the expense of the distribution area.

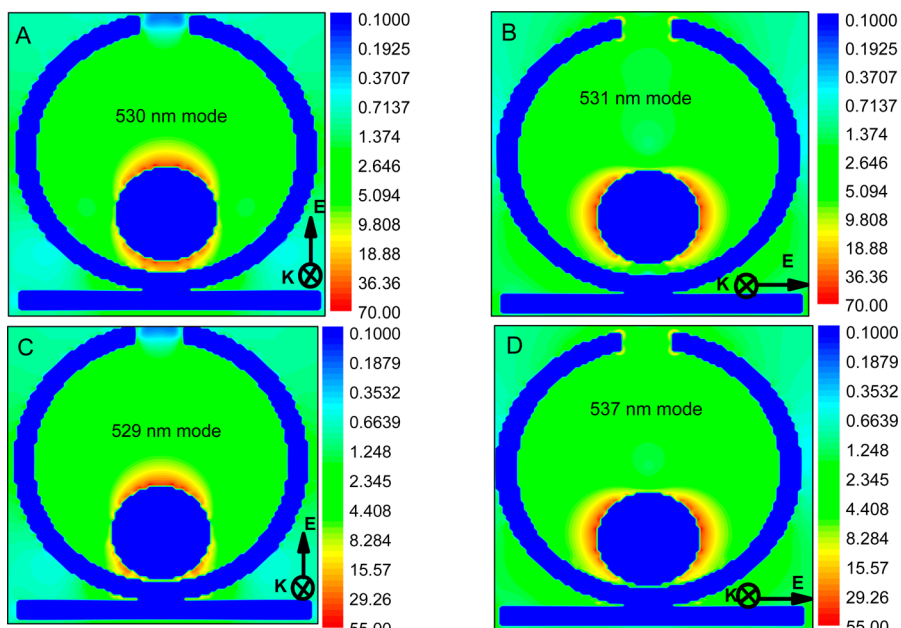


Figure 7. Plasmon field distribution contours of 90 nm gold nanorattle of 6 nm thickness and 30 nm inside gold nanosphere placed on the surface of silicon substrate, calculated by DDA at \sim 530 nm plasmon mode, when the inside separation gap between the nanosphere and the shell is 3 nm: (A) field polarized perpendicular to the surface of the substrate; (B) field polarized parallel to the surface of the substrate. At a separation distance of 0 nm: (C) perpendicular polarized light; (D) parallel polarized light. The substrate and polarization had little effect upon the intensity of the field, although they did affect the distribution.

higher energy increases and the peak position is red-shifted. The peak corresponding to the AuNSs disappears when the layer of silver nanoshell become thick enough and one peak is obtained at 413.8 and 434 nm for the small sizes nanoparticles of diameter of 16.5 and 29.8 nm, respectively. The other two gold nanospheres with larger diameter showed two plasmon peaks after coating with a thick silver nanoshell at 519 and 421.5 nm for the 53.0 nm AuNSs and 525 and 427 nm for the 65.1 AuNSs, respectively.

Characterization of Gold Nanorattles of Different Sizes. Gold nanorattles (AuNRTs) were prepared by the galvanic replacement of the silver nanoshell in Ag-AuNSs with gold hollow shell. Each gold(III) ions oxidizes three silver atoms from the Ag-AuNSs. This causes a reduction in size of the silver nanoshell and produces a gap between the AuNSs and the outer gold nanoshell. The newly prepared AuNRTs were characterized by transmission electron microscopy and by studied their optical properties.

A. TEM Imaging of the Gold Nanorattles. Parts A–D of Figure 2 show the TEM image of the AuNRTs. It is clear that the majority of the nanorattles are spherical, but few elongated particles were observed. Each AuNRT has only one internal solid AuNSs (even the elongated ones). This proves that no aggregation took place during the deposition of silver on the AuNSs or during the galvanic replacement of silver with gold. The spherical shape of the gold outer shell of the AuNRTs confirms the symmetrical growth of silver shell around the AuNSs which is replaced by gold later on. Statistical analysis of over 100 nanoparticles, collected from 4 TEM images, showed that the diameter of the outer shell of the AuNRTs are 47.4 ± 5.4 , 85.1 ± 7.3 , 143.4 ± 16.9 , and 158.6 ± 23.2 nm while the inner AuNSs are 16.5 ± 2.5 , 29.8 ± 2.4 , 3.0 ± 4.3 , 65.1 ± 11.7 nm, respectively (Figure 2A–D). The critical question that the TEM imaging cannot answer is does the AuNSs adhere to the inner surface of the outer nanoshell in the nanorattles? In order to discuss this point the bellow optical studies is carried out.

B. Studying the Structure of Gold Nanorattles by Optical Experimental and Theoretical Techniques. TEM measurement did not confirm whether the AuNSs adhere to the inner surfaces of the nanoshells or move freely. In order to study the AuNRTs system optically, we carried out DDA calculations for a 90 nm outer shell gold nanorattle with and internal AuNS of 30 nm at different separation distances from the inner surface of nanoshell of 6 nm thickness. Three holes of 10 nm \times 10 nm are generated during the simulation, and the nanorattle is placed on the center of the 90 nm \times 90 nm silicon substrate. The calculation is carried out when the incident field is polarized parallel and perpendicular to the surface of the substrate. The Experimental LSPR scattering spectra of a single AuNRT of the same dimensions were measured in dry and wet states. Very diluted solution of AuNRTs (Pico-molar) was drop casted on the surface of silicon wafer substrate. The LSPR scattering spectrum was collected for the AuNRT of SEM image in the inset of Figure 3A, immediately and after drying by a microabsorption setup. The measured spectra were compared with the theoretical results calculated at separation distances between AuNS and the inner surface of the nanoshell of 0, 3, and 15 nm in water medium when the polarization is parallel to the substrate (see Figure 3A) and perpendicular to the surface of the substrate (see Figure S2). The experimental measurement showed three plasmon peaks at 523, 638, and 842 nm, in addition to a shoulder band at 768 nm. As in case of the experimental result, the theoretical calculation showed three plasmon peaks and a shoulder except for the 0 nm separation distances, which showed four plasmon peaks and a shoulder for both polarization directions. The closest fit of the experimental result with theoretical calculation is for the AuNRT with 15 nm separation distance and the incident polarized field parallel to the surface of the substrate, since the plasmon peaks are found to be at 525, 606, and 845 nm and the shoulder is at 770 nm. The peak at 525 nm appears as a small shoulder in case of the nanorattle of 0 and 3 nm separation gap with the inner nanosphere for the parallel and perpendicular polarization directions (see the insets of Figure 3A and Figure S2). Also, the nanorattle of 0 nm separation gap has an extra peak at 690 nm when the incident field is polarized along the substrate and a sharp peak at 737 nm when the polarization is changed to be perpendicular to the surface of substrate. These LSPR scattering peaks and spectra features are not observed experimentally, which supports that idea that the inner nanosphere of the AuNRT does not adhere to their inside surface, but moves freely.

In order to confirm the idea of free movement of the inner spheres of the AuNRTs, similar measurements and calculations were repeated for the dry AuNRT (air medium is used instead of water) but with parallel polarization, since the perpendicular polarization did not match the experimental measurements. Figure 3B shows the LSPR spectrum of a single dry AuNRT measured experimentally and calculated theoretically at 0, 3, and 15 nm separation distance in air surrounding medium, when the polarized incident field is parallel to the surface of the substrate. The experimental spectrum showed two plasmon peaks at 550 and 687 nm resembling the theoretically calculated particles with 3 nm of separation having two plasmon peaks at 546 and 695 nm. Interestingly the peak at 546 nm is sharp for the nanorattle of 3 nm internal separation gap and weak shoulder is observed for the 0 and 15 nm separation as shown in the inset of Figure 3B. This suggests that the AuNSs inside the AuNRTs is free when suspended in water but adheres to

the walls after drying. Because of the presence of PVP capping ligands, the separation distance is never quite 0 nm.

Plasmon Sensing with Gold Nanorattles. The LSPR peak of the plasmonic nanoparticles shifts as the dielectric of the surrounding medium is changed making them efficient sensors. It is useful to tune the shape and the structure of the plasmonic nanoparticles to enhance their sensitivity factor. Figure 4A shows the LSPR extinction spectrum of AuNRTs with 53.0 ± 4.3 nm internal AuNSs and 143.4 ± 16.9 nm outer gold nanoshells. The LSPR extinction spectrum of AuNRTs was measured in different solvents such as methanol, water, ethanol, dichloromethane, chloroform, and carbon tetrachloride. It is observed that the LSPR peak position red-shifts as the refractive index of the solvent is increased. The LSPR extinction spectra of the other three AuNRTs were measured after dispersion in the same solvents (see Figure S3). The DDA calculations are carried out to support the experimentally measured sensitivities. In particular, the LSPR extinction spectra for an AuNRT (90 nm external, 30 nm internal sphere, 6 nm wall thickness, and 15 nm separation gap) calculated in air, water, ethanol, chloroform, and carbon tetrachloride media are shown in Figure 4B. The calculations in this case are carried out on colloidal particles without substrates. For determining the values of the sensitivity factor of the AuNRTs, the relationship between the LSPR extinction peak positions and the solvent refractive index is plotted in Figure 4C. The slope of the linear fit gives the sensitivity factor. The SFs for various sizes are shown in Table 1. The SF value is larger than what we have reported for hollow gold nanospheres (~ 300 nm/RIU). This raises the question of what does the inner gold nanosphere do in order to increase the value of the sensitivity factor of the AuNRT.

Plasmon Field Distribution on Gold Nanorattles. AuNRTs are compared with gold hollow nanospheres for better understanding the reason for the higher sensitivity factor. DDA simulations were carried out to calculate the plasmon field distribution. Parts A–D of Figure 5 shows the plasmon field distribution contour of 90 nm AuNRT of 6 nm wall thickness and 30 nm inside AuNS calculated at different plasmon modes when the inside separation gap is 15 nm. As discussed earlier, this AuNRT has four plasmon modes at 525, 606, 770 (shoulder), and 845 nm. For the 525 nm mode, the field distribution is high around the inside AuNS suggesting that this mode corresponds to the AuNS excitation. For the 606 nm mode, the field distribution is high around the holes and field strength around the inside sphere is similar to that of the 525 nm mode. This indicates that both the holes and the inside AuNSs get excited by the light of 606 nm wavelength. For the shoulder mode at 770 nm the plasmon field intensity around the hole is stronger than that around the inside AuNS, but generally the field is stronger than that for the 606 nm mode. Ultimately, the field distribution of the plasmon mode at 845 nm is strong around both the holes and the inside AuNS and comparable in intensity. Moreover, the plasmon field is distributed around the inner and outer wall of the nanoshell of the AuNRT. This supports the idea that, the whole AuNRT get excited at that wavelength. Unlike the individual AuNS and gold hollow nanospheres when they are in a separate system (Figure S4), AuNS is excited by ~ 525 nm photons only while the gold hollow nanosphere is excited at 850 nm. In AuNRT, both the nanoshell and the inside AuNS get excited by the lower energy photon at 850 nm. The high plasmon field around

the inside AuNS is the reason for the good quality of the AuNRTs in nanosensing.

In order to confirm the unique optical properties of the AuNRTs (hybrid system), the DDA calculation for the AuNRT is carried out for the plasmon field distribution at different separation gaps between AuNS and the nanoshell. Parts A and B of Figure 6 show the plasmon field distribution contour of the 90 nm AuNRT of 30 nm inside AuNS, when the separation gap between them is 0 and 3 nm at the strongest plasmon mode (~ 850 nm). The calculation of the plasmon field distribution contours for the other LSPR extinction modes at the two separation gaps are shown in Figure S5 and S6. Similar to the AuNRT simulation at 15 nm separation gap; the inside AuNS is excited by a low energy photon of 850 nm wavelength. The plasmon field intensity increases but the surface area of the field distribution decreases as the separation gap is decreased. The field distribution is distorted as the gap is decreased with higher intensity toward the adjacent sides.

In order to study the effect of substrate and the polarization of the incident field on the plasmon field intensity and distribution DDA simulations were carried out on the 90 nm AuNRT with 30 nm internal AuNSs with 0 and 3 nm separation distances, when placed on the surface of silicon substrate. The incident field is polarized along the substrate and perpendicular to the surface of the substrate. Parts A–D of Figure 7 show the plasmon filed distribution contours near the surface of the AuNRT. As observed, the substrate and the polarization do not affect the intensity of the plasmon field although the distribution and directionality of the field are disturbed.

CONCLUSION

Spherical gold nanorattles (a gold nanosphere inside a hollow gold nanosphere) were prepared with different sizes by the galvanic replacement technique. Three localized surface plasmon resonance (LSPR) extinction peaks in addition to a shoulder were recorded experimentally and calculated theoretically by the discrete dipole approximation (DDA) technique. Comparing the experimental LSPR extinction spectrum with that calculated theoretically at different separation gaps between the inside AuNSs and the inner wall of the nanorattle's shell, suggested that the inside nanosphere does not bind with the inner wall of the nanorattle. The high efficiency of AuNRTs in sensing compared with the hollow gold nanospheres is based on the presence of high plasmon field around both the inside nanosphere and the hollow outer spheres. Unlike the plasmonic nanoparticles of symmetrical shape, AuNRTs have three plasmon peaks not one as expected. This is because the internal AuNS creates asymmetry.

ASSOCIATED CONTENT

Supporting Information

Figure S1, TEM images of gold nanospheres of different sizes; Figure S2, LSPR scattering spectrum of a single AuNRT of 90 nm diameter and 6 nm wall thickness, placed on the surface of silicon substrate calculated by DDA technique at different inside separation gaps between the AuNS and the wall of the rattle; Figure S3, LSPR spectrum of gold nanorattles of different inner gold nanosphere and gold nanoshell measured when dispersed on different solvent; Figure S4, plasmon field distribution counter for 90 nm gold nanosphere of 6 nm wall thickness; and plasmon field distribution counter for 90 nm gold nanorattle of 6 nm wall thickness calculated by DDA

technique at different plasmon mode for inside AuNS located at separation gap of 0 (Figure S5) and 3 nm (Figure S6). This material is available free of charge via the Internet at <http://pubs.acs.org/>.

AUTHOR INFORMATION

Corresponding Author

^{*}(M.A.M.) E-mail: mmahmoud@gatech.edu.

Notes

The authors declare no competing financial interest.

ACKNOWLEDGMENTS

I would like to thank NSF CHE Division of Chemistry grant No. 1306269 for supporting this work.

REFERENCES

- (1) Ritchie, R. H. Plasma Losses by Fast Electrons in Thin Films. *Phys. Rev.* **1957**, *106*, 874–881.
- (2) Kreibig, U.; Vollmer, M. Optical Properties of Metal Clusters. *Springer Series in Materials Science*; Springer-Verlag: Berlin and Heidelberg, Germany, 1995; p 25.
- (3) Lee, K. S.; El-Sayed, M. A. Dependence of The Enhanced Optical Scattering Efficiency Relative to that of Absorption for Gold Metal Nanorods on Aspect Ratio, Size, End-Cap Shape, and Medium Refractive Index. *J. Phys. Chem. B* **2005**, *109*, 20331–20338.
- (4) Kelly, K. L.; Coronado, E.; Zhao, L. L.; Schatz, G. C. The Optical Properties of Metal Nanoparticles: The Influence of Size, Shape and Dielectric Environment. *J. Phys. Chem. B* **2003**, *107*, 668–677.
- (5) McFarland, A. D.; Van Duyne, R. P. Single Silver Nanoparticles as Real-Time Optical Sensors with Zeptomole Sensitivity. *Nano Lett.* **2003**, *3*, 1057–1062.
- (6) Malinsky, M. D.; Kelly, K. L.; Schatz, G. C.; Van Duyne, R. P. Nanosphere Lithography: Effect of Substrate on the Localized Surface Plasmon Resonance Spectrum of Silver Nanoparticles. *J. Phys. Chem. B* **2001**, *105*, 2343–2350.
- (7) Chen, H.; Kou, X.; Yang, Z.; Ni, W.; Wang, J. Shape- and Size-Dependent Refractive Index Sensitivity of Gold Nanoparticles. *Langmuir* **2008**, *24*, 5233–5237.
- (8) Khalavka, Y.; Becker, J.; Soennichsen, C. Synthesis of Rod-Shaped Gold Nanorattles with Improved Plasmon Sensitivity and Catalytic Activity. *J. Am. Chem. Soc.* **2009**, *131*, 1871–1875.
- (9) Mahmoud, M. A.; Chamanza, M.; Adibi, A.; El-Sayed, M. A. Effect of the Dielectric Constant of the Surrounding Medium and the Substrate on the Surface Plasmon Resonance Spectrum and Sensitivity Factors of Highly Symmetric Systems: Silver Nanocubes. *J. Am. Chem. Soc.* **2012**, *134*, 6434–6442.
- (10) Sun, Y.; Xia, Y. Increased Sensitivity of Surface Plasmon Resonance of Gold Nanoshells Compared to That of Gold Solid Colloids in Response to Environmental Changes. *Anal. Chem.* **2002**, *74*, 5297–5305.
- (11) Mahmoud, M. A.; El-Sayed, M. A. Gold Nanoframes: Very High Surface Plasmon Fields and Excellent Near-Infrared Sensors. *J. Am. Chem. Soc.* **2010**, *132*, 12704–12710.
- (12) Wang, H.; Brandl, D. W.; Le, F.; Nordlander, P.; Halas, N. J. Nanorice: A Hybrid Plasmonic Nanostructure. *Nano Lett.* **2006**, *6*, 827–832.
- (13) Faraday, M. The Bakerian Lecture: Experimental Relations of Gold (and Other Metals) to Light. *Philos. Trans. R. Soc. London* **1857**, *147*, 145–181.
- (14) Sau, T. K.; Murphy, C. J. Room Temperature, High-Yield Synthesis of Multiple Shapes of Gold Nanoparticles in Aqueous Solution. *J. Am. Chem. Soc.* **2004**, *126*, 8648–8649.
- (15) Johnson, C. L.; Snoek, E.; Ezcurdia, M.; Rodriguez-Gonzalez, B.; Pastoriza-Santos, I.; Liz-Marzan, L. M.; Hytch, M. J. Effects of Elastic Anisotropy on Strain Distributions in Decahedral Gold Nanoparticles. *Nat. Mater.* **2008**, *7*, 120–124.

- (16) Jana, N. R.; Gearheart, L.; Murphy, C. J. Wet Chemical Synthesis of High Aspect Ratio Cylindrical Gold Nanorods. *J. Phys. Chem. B* **2001**, *105*, 4065–4067.
- (17) Nehl, C. L.; Liao, H. W.; Hafner, J. H. Optical Properties of Star-Shaped Gold Nanoparticles. *Nano Lett.* **2006**, *6*, 683–688.
- (18) Millstone, J. E.; Hurst, S. J.; Metraux, G. S.; Cutler, J. I.; Mirkin, C. A. Colloidal Gold and Silver Triangular Nanoprisms. *Small* **2009**, *5*, 646–664.
- (19) Wiley, B. J.; Chen, Y. C.; McLellan, J. M.; Xiong, Y. J.; Li, Z. Y.; Ginger, D.; Xia, Y. N. Synthesis and Optical Properties of Silver Nanobars and Nanorice. *Nano Lett.* **2007**, *7*, 1032–1036.
- (20) Sun, Y. G.; Wiley, B.; Li, Z. Y.; Xia, Y. N. Synthesis and Optical Properties of Nanorattles and Multiple-Walled Nanoshells/Nanotubes Made of Metal Alloys. *J. Am. Chem. Soc.* **2004**, *126*, 9399–9406.
- (21) Sun, Y. G.; Xia, Y. N. Shape-Controlled Synthesis of Gold and Silver Nanoparticles. *Science* **2002**, *298*, 2176–2179.
- (22) Freund, P. L.; Spiro, M. Colloidal Catalysis - The Effect of Sol Size and Concentration. *J. Phys. Chem.* **1985**, *89*, 1074–1077.
- (23) Link, S.; Wang, Z. L.; El-Sayed, M. A. Alloy Formation of Gold-Silver Nanoparticles and the Dependence of The Plasmon Absorption on Their Composition. *J. Phys. Chem. B* **1999**, *103*, 3529–3533.
- (24) Harikumar, K. R.; Ghosh, S.; Rao, C. N. R. X-ray Photoelectron Spectroscopic Investigations of Cu-Ni, Au-Ag, Ni-Pd, and Cu-Pd Bimetallic Clusters. *J. Phys. Chem. A* **1997**, *101*, 536–540.
- (25) Mahmoud, M.; Saira, F.; El-Sayed, M. Experimental Evidence for the Nanocage Effect in Catalysis with Hollow Nanoparticles. *Nano Lett.* **2010**, *10*, 3764–3769.
- (26) Xie, S. F.; Lu, N.; Xie, Z. X.; Wang, J. G.; Kim, M. J.; Xia, Y. N. Synthesis of Pd-Rh Core-Frame Concave Nanocubes and Their Conversion to Rh Cubic Nanoframes by Selective Etching of the Pd Cores. *Angew. Chem. Int. Ed.* **2012**, *51*, 10266–10270.
- (27) Hu, J. T.; Odom, T. W.; Lieber, C. M. Chemistry and Physics in One Dimension: Synthesis and Properties of Nanowires and Nanotubes. *Acc. Chem. Res.* **1999**, *32*, 435–445.